

# Selective aerobic oxidation reactions via combination of photocatalytic water oxidation and enzymatic oxyfunctionalisations

Wuyuan Zhang,<sup>[a]</sup> Elena Fernández-Fueyo,<sup>[a]</sup> Yan Ni,<sup>[a]</sup> Morten van Schie,<sup>[a]</sup> Jenő Gacs,<sup>[a]</sup> Rokus Renirie,<sup>[b]</sup> Ron Wever,<sup>[b]</sup> Francesco G. Mutti,<sup>[b]</sup> Dörte Rother,<sup>[c]</sup> Miguel Alcalde,<sup>[d]</sup> Frank Hollmann\*<sup>[a]</sup>

5

<sup>[a]</sup>Department of Biotechnology, Delft University of Technology, Van der Maasweg 9, 2629HZ Delft, The Netherlands;

<sup>[b]</sup> Van't Hoff Institute for Molecular Sciences (HIMS), Faculty of Science, University of Amsterdam, Science Park 904, 1098 XH Amsterdam, The Netherlands;

10 <sup>[c]</sup> Institute of Bio- and Geosciences, IBG-1: Biotechnology, Forschungszentrum Jülich GmbH, 52425 Jülich, Germany;

<sup>[d]</sup> Department of Biocatalysis, Institute of Catalysis, CSIC, 28049 Madrid, Spain.

\*E-mail: [f.hollmann@tudelft.nl](mailto:f.hollmann@tudelft.nl)

## 15 Abstract

Peroxygenases offer versatile means to address challenges in selective oxyfunctionalisation chemistry. Despite their attractiveness, the application of peroxygenases in synthetic chemistry remains challenging due to their facile inactivation by the stoichiometric oxidant (H<sub>2</sub>O<sub>2</sub>). To address this, we show that visible light-driven, catalytic water oxidation can be used for *in situ* generation of H<sub>2</sub>O<sub>2</sub> to promote selective oxyfunctionalisation reactions catalysed by peroxygenases.

20

## Introduction

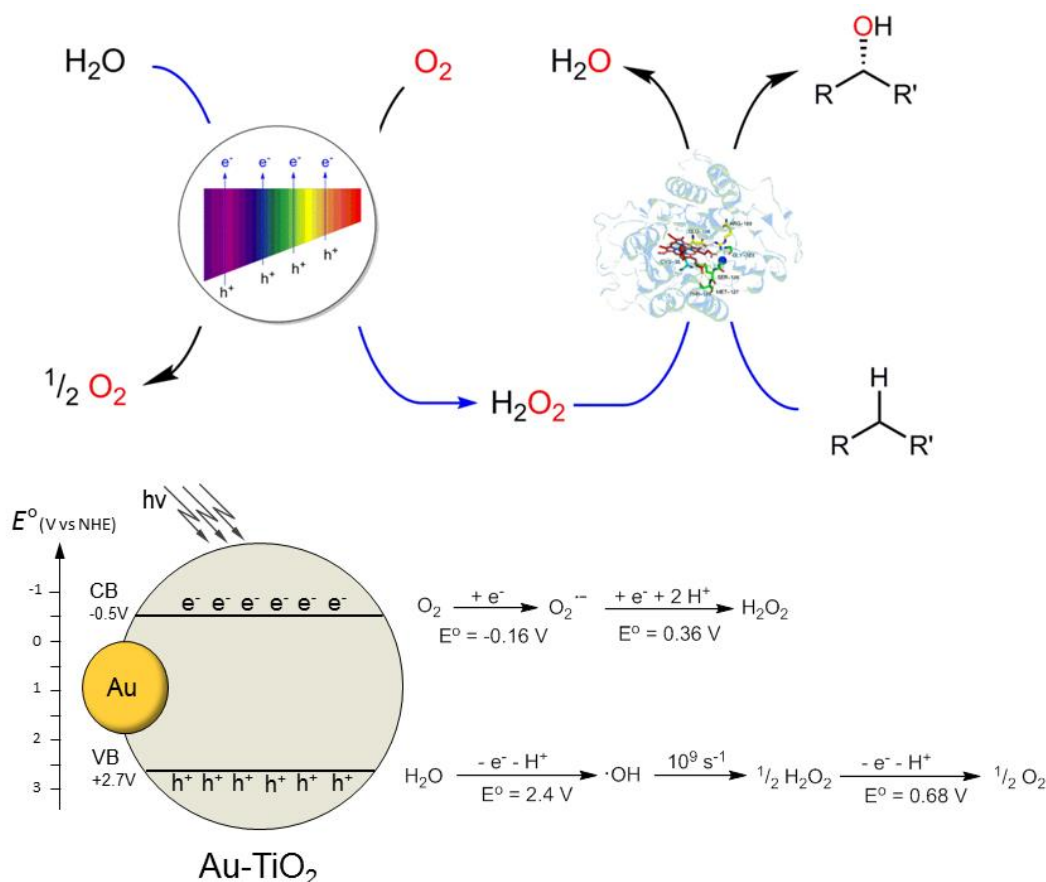
Selective oxyfunctionalisation of carbon-hydrogen bonds still represents a dream reaction in organic synthesis. 1, 2, 3, 4, 5, 6, 7 Particularly, balancing reactivity of the oxygen-transfer reagent with selectivity is largely unsolved for (in)organic catalysts while it is an inherent feature of many oxidative enzymes such as heme-dependent monooxygenases and peroxygenases. The relevance of peroxygenases (UPO for *unspecific* peroxygenase, E.C. 1.11.2.1) for selective oxyfunctionalisation reactions in preparative organic synthesis is increasing rapidly.<sup>8, 9, 10</sup> Particularly the 'novel' peroxygenases from *Agrocybe aegerita* (AaeUPO),<sup>11, 12, 13, 14</sup> *Marasmius rotula* (MroUPO)<sup>15, 16</sup> or *Coprinopsis cinerea* (CciUPO)<sup>17, 18</sup> excel in terms of substrate scope and specific activity over the well-known chloroperoxidase from *Caldariomyces fumago* (CfuUPO),<sup>19</sup> P450 monooxygenases and chemical counterparts. The very high turnover numbers (TONs) reported so far give reason to expect truly preparative-scale applications of these very promising biocatalysts. Additionally, crystal structures of AaeUPO<sup>20</sup> as well as directed evolution protocols<sup>21, 22, 23</sup> together with efficient recombinant expression systems have

30

been established in the past few years. Hence, current gaps in substrate scope, stability and/or selectivity will be closed.<sup>4, 24, 25, 26, 27, 28, 29, 30, 31</sup>

35 In contrast to P450 monooxygenases, peroxygenases do not rely on complicated and susceptible electron transport chains delivering reducing equivalents to the heme active site needed for reductive activation of molecular oxygen and therefore are not subject to the *Oxygen Dilemma*.<sup>32</sup> Rather, peroxygenases utilise H<sub>2</sub>O<sub>2</sub> directly to regenerate the catalytically active oxoferryl heme species. At the same time, however, peroxygenases suffer (like all heme-dependent enzymes) from a pronounced instability against H<sub>2</sub>O<sub>2</sub> making controlled *in situ* provision with H<sub>2</sub>O<sub>2</sub> inevitable. Today, the well-known glucose/glucose oxidase system to generate H<sub>2</sub>O<sub>2</sub> from O<sub>2</sub> prevails on lab-scale; but shows little potential for larger, preparative applications due to its poor atom-efficiency.<sup>33</sup> More efficient electron donors such as small alcohols or electrochemical sources have recently been proposed.<sup>34, 35, 36</sup>

45 Ideally, water could serve as co-substrate and electron donor for *in situ* generation of H<sub>2</sub>O<sub>2</sub>. Peroxygenase reactions are generally conducted in aqueous media ( $c(\text{H}_2\text{O}) = 55 \text{ mol L}^{-1}$ ) and the sole by-product of the water oxidation reaction is molecular oxygen. A broad variety of heterogeneous water oxidation catalysts (WOCs) have been reported in recent years that could be used for the partial oxidation of water to hydrogen peroxide.<sup>37, 38, 39, 40, 41, 42, 43, 44, 45, 46</sup> The thermodynamic driving force for this reaction is derived from (visible) light. Mostly, this approach is evaluated with respect to catalytic water splitting into H<sub>2</sub> and O<sub>2</sub>. However, under aerobic conditions, electrons liberated from water can also be transferred to O<sub>2</sub> yielding H<sub>2</sub>O<sub>2</sub>. Also, incomplete oxidation of water to H<sub>2</sub>O<sub>2</sub> can be conceived. This motivated us to evaluate catalytic, photochemical water oxidation to promote peroxygenase-catalysed, selective oxyfunctionalisation reactions (Scheme 1). For the proof-of-concept experiments Au-doped TiO<sub>2</sub> appeared promising due to its favourable redox potentials of the valence (+2.7 V) and conducting band (-0.5 V) making water oxidation ( $E^{0'} = 2.4 \text{ V}$ ) and O<sub>2</sub>-reduction ( $E^{0'} = -0.16$  V) feasible at ambient conditions (i.e. neutral pH) (Scheme 1).



**Scheme 1.** Upper: Light-driven water oxidation for the *in situ* generation of  $\text{H}_2\text{O}_2$  to promote peroxxygenase-catalysed selective hydroxylation of hydrocarbons. The electron flow is shown in blue, for clarity reasons protons are omitted from the scheme, the overall reaction is pH-neutral. Lower: band energy values for  $\text{TiO}_2$ <sup>47</sup> and elementary redox steps occurring at the  $\text{TiO}_2$ -surface. The Au-nanoparticles modulate the absorption properties (enhancing the activity with visible light).

## Results and Discussion

As model enzyme for our studies we chose an evolved expression UPO mutant from *Agrocybe aegerita*, which was recombinantly overproduced in *Pichia pastoris* (rAaeUPO) following a previously reported protocol.<sup>22</sup> The enzyme was purified to near homogeneity by a single anion exchange chromatography step (Fig S1). The enzyme preparation used herein exhibited a Reinheitszahl (Rz:  $A_{420}/A_{280}$ ) value of 1.6. As model reaction we chose the stereoselective hydroxylation of ethyl benzene to (*R*)-1-phenyl ethanol as model reaction (Figure 1). Visible-light active Au-doped  $\text{TiO}_2$  was used as photocatalysts for the proof-of-concept experiments.<sup>48, 49</sup>

Under arbitrarily chosen reaction conditions (Figure 1) we were pleased to observe significant accumulation of (*R*)-1-phenyl ethanol. Control reactions in the absence of the Au- $\text{TiO}_2$  photocatalyst or in the darkness yielded no product formation. Experiments in the absence of either the enzyme or using thermally inactivated enzyme resulted in a slow accumulation of racemic 1-phenyl ethanol (less than 0.14 mM within 24 h) and approximately the same concentrations of acetophenone. This minor background oxidation activity of the photocatalyst also explains the slightly decreased optical purity of the (*R*)-1-phenyl ethanol obtained from the

75 photobiocatalytic oxidation reactions (90% ee) as compared to traditional reaction schemes for the provision of rAaeUPO with H<sub>2</sub>O<sub>2</sub> (> 97% ee).<sup>50</sup>

Particular attention was paid to the nature of the electron donor for this reaction as in principle also other reaction components may be susceptible to TiO<sub>2</sub> oxidation and thereby serve as sacrificial electron donor for the reduction of O<sub>2</sub>. For this, the enzyme preparation contained phosphate only as buffer component to  
80 exclude possible contributions of other sacrificial hole scavengers to H<sub>2</sub>O<sub>2</sub> generation. Also experiments using immobilised enzymes were conducted to exclude rAaeUPO oxidation to promote H<sub>2</sub>O<sub>2</sub> generation. To further support the assumed water oxidation-based mechanism, we performed a range of experiments using <sup>18</sup>O labelled water as reaction mixture. The occurrence of <sup>18</sup>O-labelled (*R*)-1-phenylethanol (Figure S16) supports the proposed mechanism. Performing this experiment in the presence of ambient air (predominantly consisting  
85 of <sup>16</sup>O<sub>2</sub>) resulted in a minor incorporation of <sup>18</sup>O into the product, which predominantly contained <sup>16</sup>O. Using deaerated reaction mixtures (wherein only water oxidation can account for O<sub>2</sub>) the <sup>18</sup>O-labelled product dominated. These findings strongly support the suggested TiO<sub>2</sub>-mediated oxidation of H<sub>2</sub>O to O<sub>2</sub> coupled to TiO<sub>2</sub>-catalysed reduction of O<sub>2</sub> to H<sub>2</sub>O<sub>2</sub> finally being used by rAaeUPO for specific incorporation into ethyl benzene. Also, a contribution of H<sub>2</sub>O<sub>2</sub> originating from direct two-electron water oxidation (Scheme 1) is  
90 possible.<sup>51</sup> In any case, the above-mentioned results make us confident that water served indeed as sole source of reducing equivalents to promote the selective rAaeUPO-catalysed oxyfunctionalisation reactions.

Next, we advanced to characterise the reaction system in more detail, particularly investigating the effect of varying catalyst concentrations on the reaction system. It is worth mentioning here that, though the product concentrations shown in Figure 1 may appear low but significantly surpass the concentrations of H<sub>2</sub>O<sub>2</sub>  
95 obtained from water oxidation reported so far for Au-TiO<sub>2</sub> and other WOCs.<sup>38, 44, 52</sup> We attribute this to a H<sub>2</sub>O<sub>2</sub>-oxidation activity of the illuminated WOCs (Fig S17) eventually leading to a low steady-state concentration of H<sub>2</sub>O<sub>2</sub>.<sup>53</sup> At first sight, this may appear as a limitation for the current system, but it also enables us to maintain low, constant *in situ* concentrations of H<sub>2</sub>O<sub>2</sub> as required for efficient and robust peroxygenase catalysis.

Interestingly, the concentration of the WOC had only a minor influence on the initial rate of the  
100 reaction (Figure 1 A). We attribute this to WOC-concentration-independent *in situ* H<sub>2</sub>O<sub>2</sub> concentrations, most probably due to the simultaneous water- and H<sub>2</sub>O<sub>2</sub>-oxidation activity of the WOCs mentioned above. The WOC concentration, however, had a very significant influence on the robustness of the overall reaction. In general, no more product accumulation was observable after approx. 6 h. Varying the Au content (0.6-1.8 wt%) and particle size (2.8-7.9 nm) on the TiO<sub>2</sub> surface hardly influenced the time course of the photobiocatalytic  
105 hydroxylation reaction with the exception of plain TiO<sub>2</sub>. Here, the overall rate was approximately half of the rates obtained with Au-TiO<sub>2</sub> (Figure S9).

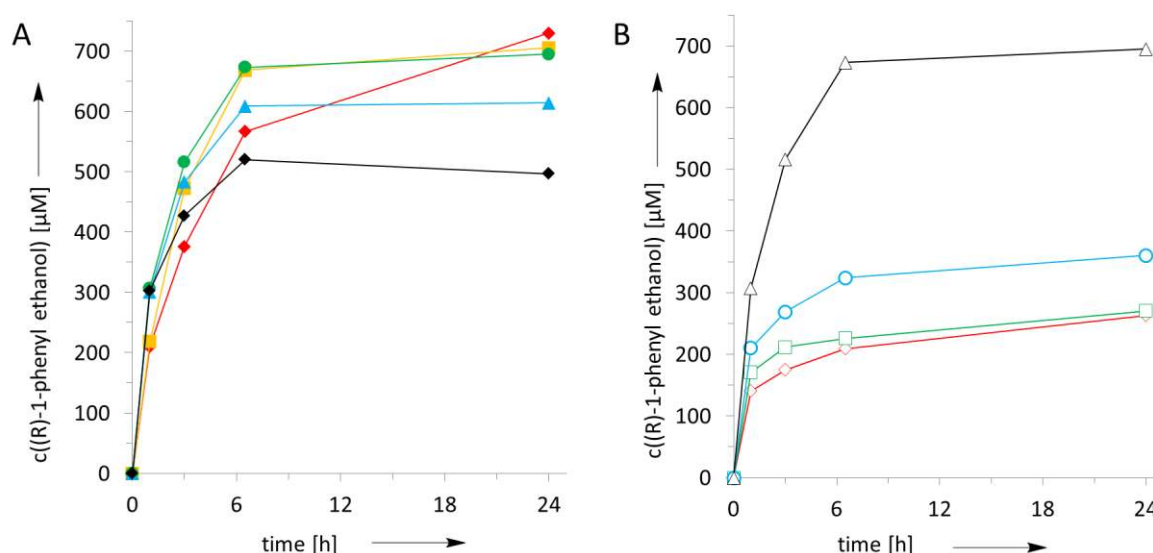
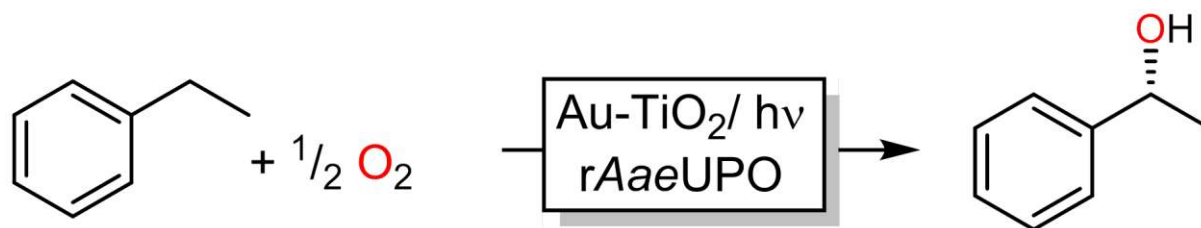


**Figure 1.** Time courses of the photochemoenzymatic hydroxylation of ethyl benzene with varying photocatalyst (A) and enzyme (B) concentrations. General conditions: reactions were performed in 60 mM phosphate buffer (pH 7.0) under visible light illumination ( $\lambda > 400$  nm),  $T = 30$  °C,  $c(\text{ethyl benzene}) = 15$  mM. A:  $c(\text{rAaeUPO}) = 350$  nM,  $c(\text{Au-TiO}_2) = 1$  gL<sup>-1</sup> (♦), 2.5 gL<sup>-1</sup> (■), 5 gL<sup>-1</sup> (●), 10 gL<sup>-1</sup> (▲), 15 gL<sup>-1</sup> (◆); B:  $c(\text{Au-TiO}_2) = 5$  gL<sup>-1</sup>,  $c(\text{rAaeUPO}) = 10$  nM (♦), 50 nM (□), 150 nM (○), 300 nM (△).

In contrast, the enzyme concentration directly influenced the overall reaction rate (Figure 1 B) and a linear dependency of the initial (*R*)-1-phenyl ethanol accumulation on the concentration of *rAaeUPO* applied was observed. However, again, the reactions ceased after 6-7 h.

Apparently, the robustness of the overall reaction (as judged from the accumulation of (*R*)-1-phenyl ethanol) correlated with the ratio of photo- and bio-catalyst. We hypothesised that *rAaeUPO* may be inactivated by the Au-TiO<sub>2</sub>-WOC. It should be mentioned here, that in the experiments reported so far, only TiO<sub>2</sub> mostly composed of anatase (91.1%) had been used as WOC. Given the rather hydrophilic surface of anatase TiO<sub>2</sub>, adsorption of the glycoprotein *rAaeUPO* (with a glycosylation degree of 30 %) <sup>22</sup> appears likely. Therefore, we performed a range of control experiments to shed light on the inactivation of the biocatalyst: incubation of the enzyme with the photocatalyst in the darkness resulted in a minor reduction of its catalytic activity as compared to the same experiment in the presence of light (Figure 2). Therefore, we conclude that adsorption of *rAaeUPO* to the photocatalyst *per se* does not lead to inactivation of the enzyme.

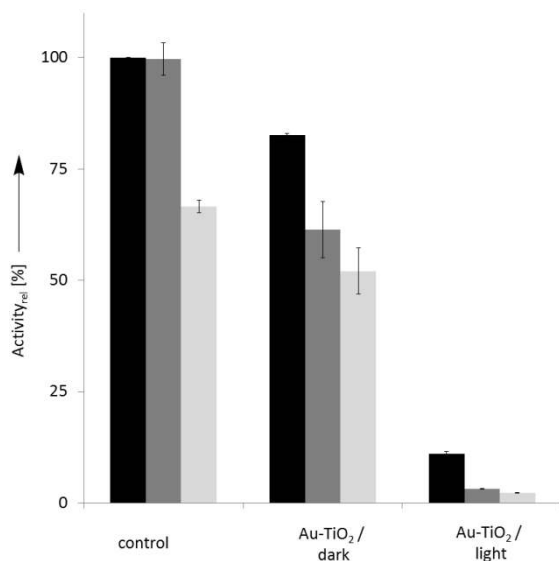


**Figure 2.** Residual rAaeUPO activity after incubation in the presence of the photocatalyst for 1 (black), 5 (dark grey) and 24 h (light grey). General conditions: phosphate buffer (60 mM, pH 7.0), T= 30 °C, c(anatase Au-TiO<sub>2</sub>) = 0 (control, under illumination) or 10 gL<sup>-1</sup>, c(rAaeUPO) = 150 nM. The samples were either kept in the darkness or illuminated under visible light illumination ( $\lambda > 400$  nm). At intervals, samples were withdrawn from the incubation mixtures and analysed for peroxygenase activity.

We hypothesised that reactive oxygen species (ROS) generated at the surface of the water oxidation catalyst<sup>54</sup> may account for this observation via oxidative inactivation of the enzyme. In fact, using the spin trap technique in electron paramagnetic resonance spectroscopy, significant amounts of mainly hydroxyl (HO•) radicals ( $a_H = 1.495$  mT;  $g = 2.0050$ ) could be detected in illuminated anatase Au-TiO<sub>2</sub> samples (Figure 3 A).<sup>54</sup> These hydroxyl radicals may originate from water oxidation (Scheme 1), from the reaction of superoxide ( $\bullet\text{O}_2^-$ , from O<sub>2</sub> reduction) or other steps in the complex redox chemistry of ROS.<sup>55, 56</sup> Though more detailed mechanistic studies will be necessary to fully understand this inactivation mechanism, we hypothesise a major role of the hydroxyl radical over the superoxide radical. First, addition of superoxide dismutase did not improve the robustness of the overall reaction. Second,  $\bullet\text{O}_2^-$  should react with native peroxygenase leading to the formation of the so-called Compound III of the catalytic cycle, for which we have not found any spectroscopic evidence (no characteristic absorption peak at 625 nm, Figure S10).<sup>57</sup>

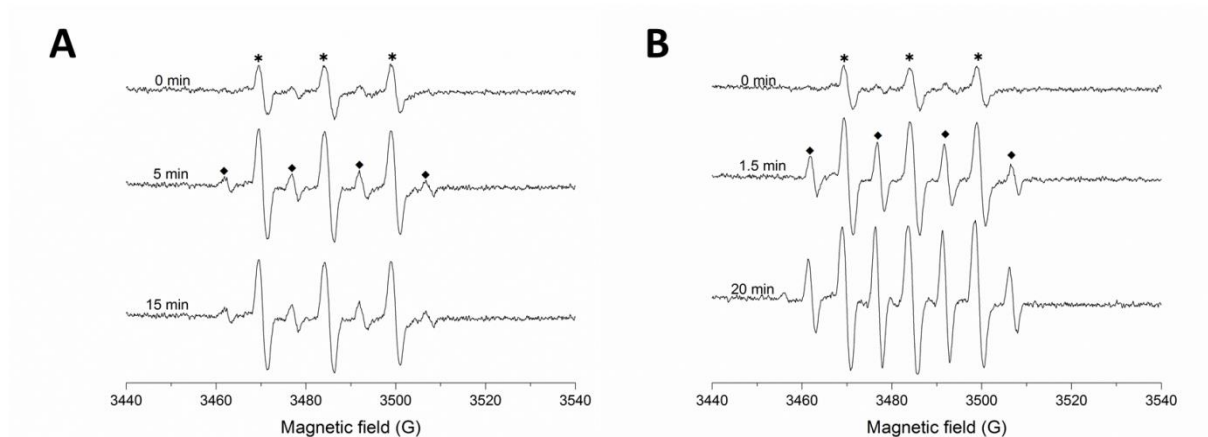


**Figure 3.** Electron paramagnetic resonance (EPR) spectra recorded during the illumination of anatase (A) and rutile (B) Au-TiO<sub>2</sub> in water. Signals marked with asterisk belong to the existing oxidation product of DMPO, 5,5-dimethyl-2-oxopyrroline-1-oxyl (DMPOX);<sup>58</sup> signals marked with solid diamonds belong to the spin-adduct •DMPO-OH, which is not overlapping the signals of DMPOX and therefore provides sufficient quality for analysis. Reaction condition: Au-TiO<sub>2</sub> = 5.0 mg mL<sup>-1</sup>, c(DMPO) = 30 mM, RT,  $h\nu > 400$  nm. DMPO = 5,5-Dimethyl-1-pyrroline *N*-oxide.

Given the rather short half-life time of hydroxyl radicals (approx.  $10^{-9}$  s in aqueous media) we envisioned that simple spatial separation of the WOC (at which's surface the HO• radicals are being formed) and the biocatalyst may circumvent this limitation. Therefore, we evaluated (1) spatial separation of anatase Au-TiO<sub>2</sub> from rAaeUPO using immobilised enzymes and (2) avoiding rAaeUPO adsorption to the WOC surface by using hydrophobic surfaces.

To achieve physical separation of the WOC and rAaeUPO, we covalently immobilised the latter to a poly(methyl methacrylate) resin activated by glutardialdehyde. Covalent linkage to the spacer unit occurred through imine formation with surface-exposed lysine residues (see SI for more detailed information). To test the second option, i.e. avoidance of enzyme adsorption by less hydrophilic WOC surfaces, rutile Au-TiO<sub>2</sub> was evaluated. Rutile exhibits a far more hydrophobic surface as compared to the previously used anatase catalyst. This is corroborated also by the lack of the characteristic IR-absorptions of surface-bound H<sub>2</sub>O and Ti-OH at 3422 and 1632 cm<sup>-1</sup>, respectively (Figure S19). This leads to the assumption that the heavily glycosylated rAaeUPO may be less prone to adsorption to rutile than to anatase surfaces. Hence, while the photoelectrochemical properties (i.e. the redox potential and energy levels of conducting- and valence band)<sup>59</sup> of both crystal phases are comparable, rutile should be preferable due to its expected lower adsorption tendency for proteins. Indeed, rAaeUPO adsorbed approximately 10 times less to rutile as compared to anatase catalyst (Figures S11 & S 12). Furthermore, this effect does not appear to be limited to glycoproteins such as rAaeUPO as also a bacterial enzyme (the old yellow enzyme homologue from *Bacillus subtilis*, YqjM)<sup>60</sup> showed a similar adsorption behaviour as rAaeUPO (Figure S13). Overall, both strategies appeared to be suitable to minimise oxidative inactivation of rAaeUPO at the photocatalyst surface and therefore should lead to more

robust photobiocatalytic hydroxylation reactions. Figure 4 compares the time courses of these catalytic systems.

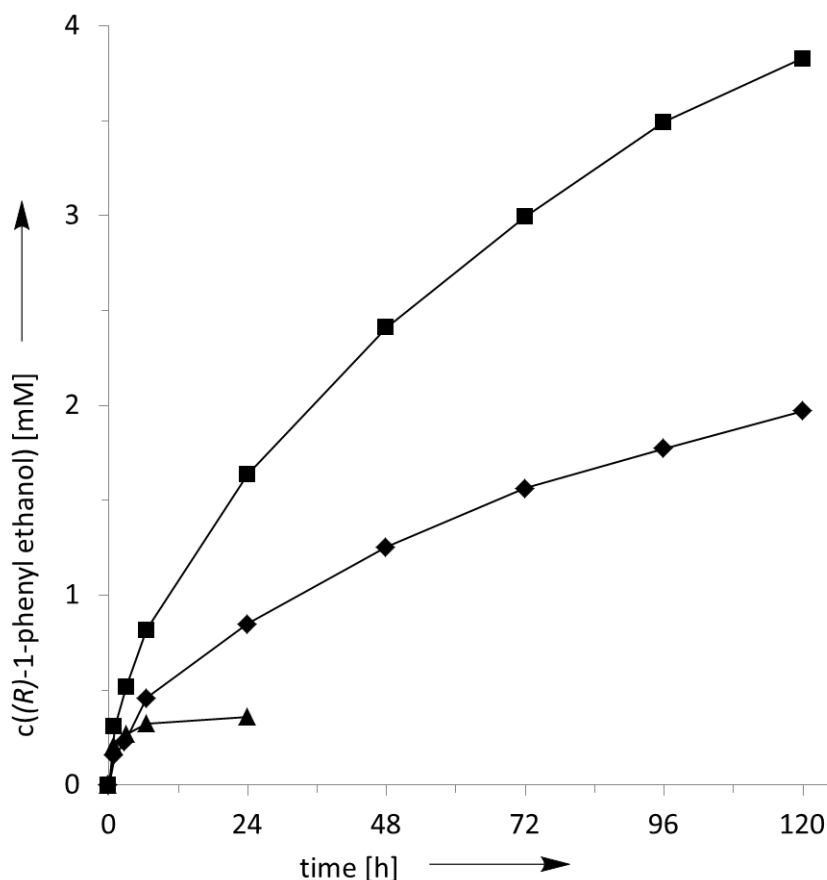


**Figure 4.** Time courses of the photobiocatalytic hydroxylations of ethyl benzene using the original reaction setup with dissolved *rAaeUPO* and anatase-Au-TiO<sub>2</sub> (▲) and systems with reduced interaction between *rAaeUPO* and the Au-TiO<sub>2</sub> by using immobilised enzyme (◆) or by using hydrophobic rutile-Au-TiO<sub>2</sub> (■). General conditions: *c*(*rAaeUPO*) = 150 nM (dissolved) 120 nM (immobilised), *c*(Au-TiO<sub>2</sub>) = 5 g L<sup>-1</sup>, *c*(ethyl benzene)<sub>0</sub> = 15 mM ethyl benzene in 60 mM phosphate buffer (pH 7.0) under visible light illumination ( $\lambda > 400$  nm).

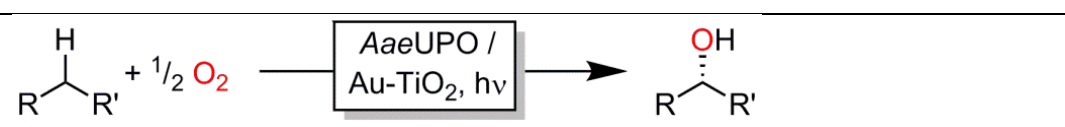
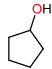
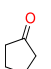
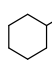
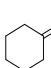
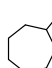
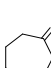
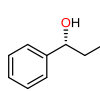
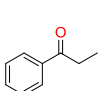
In both cases steady product accumulation was observed for at least 120 h thereby representing a more than 20-fold increase of the robustness as compared to the starting conditions (Figure 4 ▲). Consequently, also the turnover number of the enzyme increased from approx. 2000 using dissolved enzyme and anatase-Au-TiO<sub>2</sub> to more than 16000 or 21000 using immobilised *rAaeUPO* (Figure 4 ◆) or rutile-Au-TiO<sub>2</sub> (Figure 4 ■), respectively. The latter system also provided (*R*)-1-phenyl ethanol in much higher optical purity (>98% ee) as compared to the starting conditions. The reaction using immobilised *rAaeUPO* was considerably slower than the reaction using free *rAaeUPO* and rutile-Au-TiO<sub>2</sub>. This may, at least to some extent, be attributed to diffusion limitations originating from the double heterogeneous character of the catalysts. Also, partial loss of enzyme activity as a consequence of the immobilisation may contribute to this.<sup>61, 62</sup> Systematic immobilisation studies with *rAaeUPO* are currently ongoing to clarify this.

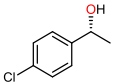
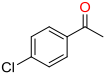
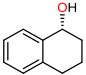
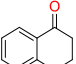
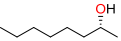
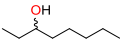


The average turnover frequency of rAaeUPO of 2.9 min<sup>-1</sup> (average over 4 days) indicates that there is room for improving the efficiency of this reaction system. Indeed, increasing the rutile-Au-TiO<sub>2</sub> concentration linearly increased the initial rate of the overall reaction (Figure S20). Surprisingly, an EPR investigation of the rutile-Au-TiO<sub>2</sub> catalysed water oxidation (Figure 3 B) revealed that this catalyst generates significantly higher amounts of •HO radicals than anatase-Au-TiO<sub>2</sub>. In fact, as already stated, a higher amount of superoxide may be formed by rutile Au-TiO<sub>2</sub>. At first sight this is in contrast to the higher compatibility of rutile-Au-TiO<sub>2</sub> with the enzymes investigated. It may, however, be rationalised by the poor adsorption tendency of proteins to the rutile-TiO<sub>2</sub> surface and the very short half life time of the hydroxyl radical resulting in very short diffusion distances.<sup>63, 64</sup>

Encouraged by these promising results, we further explored the product scope of the photochemoenzymatic hydroxylation reaction using dissolved rAaeUPO and rutile-Au-TiO<sub>2</sub>. As shown in Table 1, a broad range of aliphatic and aromatic compounds was converted into the corresponding alcohols. The enantioselectivities and relative activities corresponded to the values reported previously indicating that the natural reactivity and selectivity of the enzyme were not impaired.<sup>65, 66</sup> Similar results were also observed in the system utilising anatase-Au-TiO<sub>2</sub> and immobilised enzyme (Table S2). It is worth mentioning here that the current reactor setup chosen for these experiments suffers from severe issues in mass balance of the reagents due to their volatility. Hence, many examples from Table 1, though exhibiting seemingly low yields actually represent full conversion of all starting material. Reaction setups avoiding direct contact of the reaction mixtures with ambient atmosphere will minimise this loss of reagents due to evaporation. Also semipreparative-scale reactions proofed to be feasible with this setup (Figures S39-S41). Hence, approx. 110 mg of highly enantioenriched (ee = 97.4%, 31% isolated yield) (*R*)-1-phenyl ethanol was produced.

**Table 1.** Substrate scope of the photobiocatalytic hydroxylation reaction.<sup>[a]</sup>

							
Entry	product	mM <sup>[b]</sup>	ee [%] <sup>[b]</sup>	Other products	mM <sup>[b]</sup>	Yield, % <sup>[b]</sup>	TON, 10 <sup>3</sup> <sup>[b]</sup>
1		4.1	/		0.5	45.2	30.1
2		4.2	/		0.1	43.1	28.7
3		2.6	/		0.1	26.7	17.8
4		2.3	>99		0.5	28.2	18.8

5		3.6	95.2		1.0	45.8	30.5
6		5.0	75.0		0.8	58.2	38.8
7		0.3	78.5		0.2	4.8	3.2

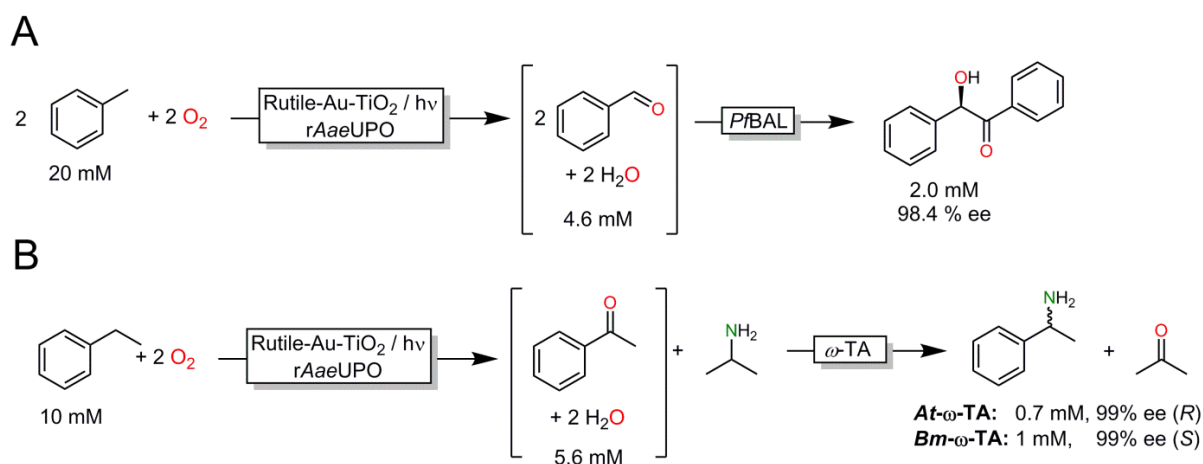
<sup>[a]</sup> Conditions:  $c(\text{substrate})_0 = 10.0 \text{ mM}$ ,  $c(\text{rutile Au-TiO}_2) = 10 \text{ g L}^{-1}$ ,  $c(\text{rAaeUPO}) = 150 \text{ nM}$  (dissolved), in phosphate buffer (pH 7.0, 60 mM),  $T = 30 \text{ }^\circ\text{C}$ , 70 h, visible light illumination ( $\lambda > 400 \text{ nm}$ ). n.d. = not determined. <sup>[b]</sup> based on the concentration of both products.

220 The regioselectivity of all reactions was very high except for entry 7 where  $\omega$ -2 and  $\omega$ -3 hydroxylation products were observed. This observation is in line with previous reports on AaeUPO-selectivity towards linear alkanes.<sup>67</sup>

225 Generally, the only by-product observed was the ‘overoxidation’ product, i.e. the corresponding ketone. We suspected WOC-catalysed further oxidation of the primary rAaeUPO-product ((R)-1-phenyl ethanol) to account for this. Indeed, the concentration of acetophenone linearly increased with increasing concentrations of Au-TiO<sub>2</sub> (Table S3). Hence, the overoxidation degree can be controlled by adjusting the concentration of the photocatalyst.

230 The dual activity of the photocatalyst (water- and alcohol oxidation) motivated us to evaluate more elaborate photochemoenzymatic cascades to extend the product scope beyond (chiral) alcohols. In particular, we coupled the photochemoenzymatic oxidation of toluene to benzaldehyde to an enzymatic benzoin condensation using the benzaldehyde lyase from *Pseudomonas fluorescens* (PfbAL) (Scheme 2 A).<sup>68, 69</sup> Also, acetophenone, formed by the photoenzymatic oxyfunctionalisation of ethyl benzene was submitted to a reductive amination using the  $\omega$ -transaminases from *Aspergillus terreus* (R-selective, At- $\omega$ -TA) and *Bacillus megaterium* (S-selective, Bm- $\omega$ -TA) (Scheme 2 B).<sup>70, 71</sup> Both cascades were performed in a one-pot-two-step fashion, i.e. the photochemoenzymatic oxidation to the corresponding aldehyde or ketone was performed first, followed by addition of the biocatalysts needed for the second transformation (details can be found in SI). Recently, Flitsch and coworkers reported a similar transformation (ethyl benzene to enantiomerically pure (R)- or (S)-1-phenyl ethyl amine) attaining very similar product titers.<sup>72</sup> It is worth mentioning that also a one-pot-one-step procedure was possible in case of cascade B, albeit at somewhat lower product yields (0.7 mM, 37 % ee and 0.5 mM, 99 % ee for (R)- and (S)-1-phenyl ethyl amine, respectively).

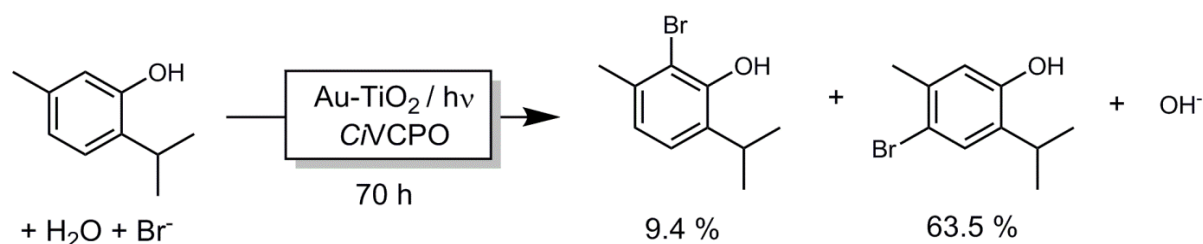
240



**Scheme 2.** Photochemoenzymatic cascade reaction for the transformation of toluene to (*R*)-benzoin (**A**) and ethyl benzene to (*R*)- or (*S*)-1-phenyl ethyl amine (**B**). Conditions: cascade A: c(toluene) = 20.0 mM, c(rutile Au-TiO<sub>2</sub>) = 30 g L<sup>-1</sup>, c(rAaeUPO) = 150 nM in phosphate buffer (pH 7.0, 60 mM), T = 30 °C, 96 h, visible light illumination ( $\lambda > 400$  nm). In the second step, 100  $\mu$ L of mixture in phosphate buffer (500 mM, pH 8.5) containing 5 mM of thiaminpyrophosphate (TPP), 25 mM of MgCl<sub>2</sub> and 10 mg of crude cell extract containing *Pf*BAL were added. Cascade B: c(ethyl benzene) = 10.0 mM, c(rutile Au-TiO<sub>2</sub>) = 30 g L<sup>-1</sup>, c(rAaeUPO) = 150 nM in phosphate buffer (pH 7.0, 60 mM), T = 30 °C, 96 h. In the second step, 105  $\mu$ L of isopropylamine, 130  $\mu$ L of phosphoric acid (5 M), 100  $\mu$ L of pyridoxal phosphate (PLP, 10 mM) and 10 mg of crude cell extract containing  $\omega$ -transaminase were added. The pH of above mixture was adjusted to approx. 9.0. The dilution factor of the reaction system was 1.0/1.335 = 0.75. After the first steps under illumination and initiation of the second steps the resulting reaction mixture of both cascades was shaken at 30 °C for 40 h in the darkness

These results demonstrate that the proposed photochemoenzymatic cascades enable synthesis of a broader range of value-added products (chiral alcohols, amines and acyloins) from simple starting materials. While these reactions undoubtedly still need further improvement to reach preparative feasibility, they nevertheless demonstrate the principal feasibility and broad product scope of the envisioned photochemoenzymatic cascade reactions.

The proposed *in situ* H<sub>2</sub>O<sub>2</sub> generation system can also be applied to other peroxidases such as the V-dependent haloperoxidase from *Curvularia inaequalis* (CVCPO).<sup>73, 74, 75, 76</sup> Gratifyingly, the CVCPO-catalysed halogenation of thymol proceeded smoothly yielding 2- and 4-bromothymol with more than 70 % conversion (Scheme 3). The product distribution was comparable to previous haloperoxidase-catalysed halogenation reactions.<sup>77, 78, 79, 80, 81</sup> In the absence of either CVCPO, rutile-Au-TiO<sub>2</sub> or light, no conversion of thymol was observed. It is also worth mentioning that again rutile-Au-TiO<sub>2</sub> gave better results than anatase-Au-TiO<sub>2</sub> with this enzyme under otherwise identical conditions.



**Scheme 3.** Photochemoenzymatic halogenation of thymol. Conditions: c(rutile Au-TiO<sub>2</sub>) = 5 g L<sup>-1</sup>, c(CVCPO) = 150 nM, c(thymol) = 3 mM, c(KBr) = 6 mM, c(Na<sub>3</sub>VO<sub>4</sub>) = 50  $\mu$ M in 1.0 mL citrate buffer (50 mM, pH 5.0) T = 30 °C, t = 70 h. The reaction mixture was irradiated by visible light ( $\lambda > 400$  nm).

So far, we have focussed on TiO<sub>2</sub>-based photocatalysts. Photocatalysis, however, is an extremely dynamic area of research and novel, potentially useful, WOCs are reported on an almost weekly basis. Therefore, we finally evaluated the scope of different WOCs for the in situ generation of H<sub>2</sub>O<sub>2</sub> to promote peroxygenase-catalysed hydroxylation reactions. Amongst them visible light-active Au-BiVO<sub>4</sub><sup>38</sup> and g-C<sub>3</sub>N<sub>4</sub><sup>82</sup> showed some promising characteristics (Figure S43). The product formation with Au-BiVO<sub>4</sub> as photocatalyst was rather modest. g-C<sub>3</sub>N<sub>4</sub> exhibited a higher product formation rate together with a pronounced 'overoxidation activity' (approx. 10 times higher than Au-TiO<sub>2</sub> under comparable conditions).<sup>83</sup> Therefore, the latter catalyst may be particularly suitable for further photobiocatalytic cascades.

Finally, recently described carbon nano dot (CND) photocatalysts caught our attention as easy-to-prepare and biocompatible photocatalysts.<sup>84, 85, 86</sup> As CND-mediated reduction of molecular oxygen to H<sub>2</sub>O<sub>2</sub> is impaired<sup>84</sup> we used riboflavin monophosphate (flavin mononucleotide, FMN) as co-catalyst for the generation of H<sub>2</sub>O<sub>2</sub> (Figure 5). Visible light illumination of a mixture of CND and FMN in deaerated phosphate buffer resulted in fast and complete reduction of FMN as judged by the decrease of the characteristic absorption band of FMN<sup>Ox</sup> at 450 nm (Figure 5 A). Exposure to ambient atmosphere resulted in complete restoration of this absorbance indicating aerobic reoxidation of FMN<sup>Red</sup> yielding H<sub>2</sub>O<sub>2</sub>.

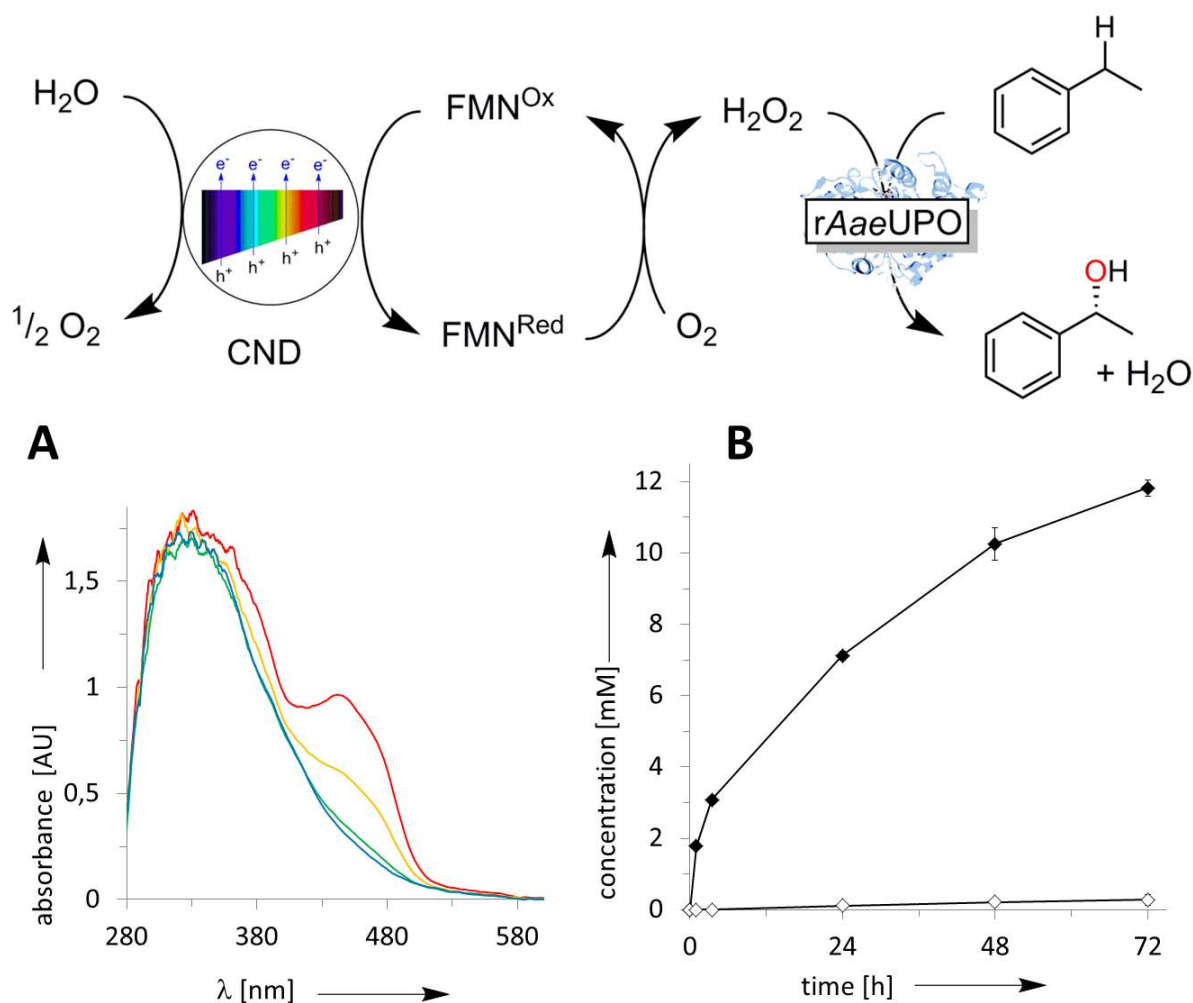


**Figure 5.** Photobiocatalytic hydroxylation of ethyl benzene to (*R*)-1-phenyl ethanol using carbon nano dot photocatalysts and FMN-cocatalysts. Upper: Proposed reaction scheme. A: UV-spectroscopic investigation of the photocatalytic reduction of FMN and B: exemplary time course of the complete reaction system. General conditions: A: The reaction was performed under anaerobic conditions in a glove box. Reaction condition: [CND] = 1 g L<sup>-1</sup> and [FMN] = 0.05 mM in phosphate buffer pH 7.0 (60 mM),  $\lambda$  = 450 nm, at intervals (0 (red), 5 (orange), 15 (green) and 30 (blue) min) the reaction mixtures were analysed by UV/Vis spectroscopy; B: [rAaeUPO] = 120 nM, [ethyl benzene] = 15 mM, [CD] = 5 g L<sup>-1</sup> and [FMN] = 0.1 mM in 60 mM phosphate buffer (pH 7.0) under visible light irradiation ( $\lambda$  > 400 nm).

Next, we tested the photocatalytic reduction of FMN and its aerobic,  $H_2O_2$ -forming reoxidation to promote rAaeUPO-catalysed hydroxylation. Experiments in the absence of either CND or FMN gave no significant product formation whereas the whole system produced enantiomerically pure (*R*)-1-phenyl ethanol (98 % ee) (Figure 5 B). Compared to the previously used Au-TiO<sub>2</sub> the overall reaction rates were significantly higher as compared by the initial rates of 0.16 mM h<sup>-1</sup> and 0.81 mM h<sup>-1</sup> for Au-TiO<sub>2</sub> and CND, respectively. Hence, already under non-optimised conditions, almost 100000 turnovers for rAaeUPO and more than 100 for FMN were estimated. Similar results were achieved under the same conditions for the hydroxylation of cyclohexane (Figure S44). It is also worth noting that the overoxidation rate was reduced significantly.

Overall, we have combined photochemical water oxidation-catalysis with peroxygenase-catalysis to achieve visible light-driven, aerobic oxidation of hydrocarbons. Combined with further (enzymatic) reaction

steps this method gives access to a broad range of functionalised building blocks starting from simple alkanes. Admittedly, the system reported here falls short in terms of space-time-yields to be economical or environmentally benign.<sup>87, 88</sup> But the catalytic turnover achieved for the biocatalyst compares well with the state-of-the-art in peroxygenase reactions and surpasses the performance of the established P450 monooxygenases and chemical catalysts (Table S6). Further improvements may be expected in the near future from optimised reaction schemes, particularly from more active WOCs.

## Acknowledgements

Financial support by the European Research Council (ERC Consolidator Grant No. 648026) is gratefully acknowledged. The authors thank Ben Norder for XRD, Dr. Wiel H. Evers for TEM and Prof. Fred Hagen for EPR measurements. The authors also thank Dr. Sandy Schmidt for the preparation of benzaldehyde lyase, Dr. Milja Pesic for the preparation of YqjM and Dr. Tanja Knaus for the preparation of  $\omega$ -transaminases. F.G.M. received funding as a European Research Council (ERC) Starting Grant Fellow (grant agreement 638271).

## References

1. Yuan CX, Liang Y, Hernandez T, Berriochoa A, Houk KN, Siegel D. Metal-free oxidation of aromatic carbon-hydrogen bonds through a reverse-rebound mechanism. *Nature* 2013, **499**(7457): 192-196.
2. Osberger TJ, Rogness DC, Kohrt JT, Stepan AF, White MC. Oxidative diversification of amino acids and peptides by small-molecule iron catalysis. *Nature* 2016, **537**(7619): 214-219.
3. Narayan ARH, Jimenez-Oses G, Liu P, Negretti S, Zhao WX, Gilbert MM, *et al.* Enzymatic hydroxylation of an unactivated methylene C-H bond guided by molecular dynamics simulations. *Nat. Chem.* 2015, **7**(8): 653-660.
4. Kille S, Zilly FE, Acevedo JP, Reetz MT. Regio- and stereoselectivity of P450-catalysed hydroxylation of steroids controlled by laboratory evolution. *Nat. Chem.* 2011, **3**(9): 738-743.
5. Kudrik EV, Afanasiev P, Alvarez LX, Dubourdeaux P, Clemancey M, Latour JM, *et al.* An N-bridged high-valent diiron-oxo species on a porphyrin platform that can oxidize methane. *Nat. Chem.* 2012, **4**(12): 1024-1029.
6. Kamata K, Yonehara K, Nakagawa Y, Uehara K, Mizuno N. Efficient stereo- and regioselective hydroxylation of alkanes catalysed by a bulky polyoxometalate. *Nat. Chem.* 2010, **2**(6): 478-483.
7. Groves JT. Enzymatic C-H bond activation: Using push to get pull. *Nat. Chem.* 2014, **6**(2): 89-91.
8. Hofrichter M, Ullrich R. Oxidations catalyzed by fungal peroxygenases. *Curr. Opin. Chem. Biol.* 2014, **19**(0): 116-125.
9. Wang Y, Lan D, Durrani R, Hollmann F. Peroxygenases en route to becoming dream catalysts. What are the opportunities and challenges? *Curr. Opin. Chem. Biol.* 2017, **37**: 1-9.
10. Bormann S, Gomez Baraibar A, Ni Y, Holtmann D, Hollmann F. Specific oxyfunctionalisations catalysed by peroxygenases: opportunities, challenges and solutions. *Catal. Sci. Technol.* 2015, **5**: 2038-2052.

11. Wang X, Peter S, Ullrich R, Hofrichter M, Groves JT. Driving Force for Oxygen-Atom Transfer by Heme-Thiolate Enzymes. *Angew. Chem. Int. Ed.* 2013, **52**(35): 9238–9241.
- 350 12. Piontek K, Ullrich R, Liers C, Diederichs K, Plattner DA, Hofrichter M. Crystallization of a 45 kDa peroxygenase/peroxidase from the mushroom *Agrocybe aegerita* and structure determination by SAD utilizing only the haem iron. *Acta Crystallogr. F-Struct. Biol. Cryst. Commun.* 2010, **66**: 693-698.
- 355 13. Ullrich R, Liers C, Schimpke S, Hofrichter M. Purification of homogeneous forms of fungal peroxygenase. *Biotechnol. J.* 2009, **4**: 1619-1626.
14. Ullrich R, Nüske J, Scheibner K, Spantzel J, Hofrichter M. Novel haloperoxidase from the agaric basidiomycete *Agrocybe aegerita* oxidizes aryl alcohols and aldehydes. *Appl. Environ. Microbiol.* 2004, **70**(8): 4575-4581.
- 360 15. Olmedo A, Aranda C, del Rio JC, Kiebitz J, Scheibner K, Martinez AT, *et al.* From alkanes to carboxylic acids: terminal oxygenation by a fungal peroxygenase. *Angew. Chem. Int. Ed.* 2016, **55**(40): 12248-12251.
- 365 16. Grobe G, Ullrich R, Pecyna MJ, Kapturska D, Friedrich S, Hofrichter M, *et al.* High-yield production of aromatic peroxygenase by the agaric fungus *Marasmius rotula*. *AMB Express* 2011, **1**(1): 31.
17. Babot ED, del Río JC, Kalum L, Martínez AT, Gutiérrez A. Oxyfunctionalization of aliphatic compounds by a recombinant peroxygenase from *Coprinopsis cinerea*. *Biotechnol. Bioeng.* 2013, **110**: 2323–2332.
- 370 18. Lucas F, Babot ED, Canellas M, del Rio JC, Kalum L, Ullrich R, *et al.* Molecular determinants for selective C-25-hydroxylation of vitamins D-2 and D-3 by fungal peroxygenases. *Catal. Sci. Technol.* 2016, **6**(1): 288-295.
- 375 19. van Rantwijk F, Sheldon RA. Selective oxygen transfer catalysed by heme peroxidases: synthetic and mechanistic aspects. *Curr. Opin. Biotechnol.* 2000, **11**(6): 554-564.
20. Piontek K, Strittmatter E, Ullrich R, Gröbe G, Pecyna MJ, Kluge M, *et al.* Structural basis of substrate conversion in a new aromatic peroxygenase: P450 functionality with benefits. *J. Biol. Chem.* 2013, **288**: 34767-34776.
- 380 21. Molina-Espeja P, Canellas M, Plou FJ, Hofrichter M, Lucas F, Guallar V, *et al.* Synthesis of 1-Naphthol by a Natural Peroxygenase Engineered by Directed Evolution. *ChemBioChem* 2016, **17**(4): 341-349.
- 385 22. Molina-Espeja P, Ma S, Mate DM, Ludwig R, Alcalde M. Tandem-yeast expression system for engineering and producing unspecific peroxygenase. *Enz. Microb. Technol.* 2015, **73–74**(0): 29-33.
- 390 23. Molina-Espeja P, Garcia-Ruiz E, Gonzalez-Perez D, Ullrich R, Hofrichter M, Alcalde M. Directed Evolution of Unspecific Peroxygenase from *Agrocybe aegerita*. *Appl. Environ. Microbiol.* 2014, **80**(11): 3496-3507.
24. Bornscheuer UT, Huisman GW, Kazlauskas RJ, Lutz S, Moore JC, Robins K. Engineering the third wave of biocatalysis. *Nature* 2012, **485**(7397): 185-194.
- 395 25. Turner NJ. Directed evolution drives the next generation of biocatalysts. *Nat. Chem. Biol.* 2009, **5**(8): 568-574.
26. Wang J, Lonsdale R, Reetz MT. Exploring substrate scope and stereoselectivity of P450 peroxygenase OleTJE in olefin-forming oxidative decarboxylation. *Chem. Commun.* 2016, **52**: 8131-8133.
- 400 27. Roiban GD, Agudo R, Reetz MT. Cytochrome P450 catalyzed oxidative hydroxylation of achiral organic compounds with simultaneous creation of two chirality centers in a single C-H activation step. *Angew. Chem. Int. Ed.* 2014, **53**(33): 8659-8663.

- 405 28. Reetz MT. Biocatalysis in organic chemistry and biotechnology: past, present, and future. *J. Am. Chem. Soc.* 2013, **135**(34): 12480-12496.
29. Glieder A, Farinas ET, Arnold FH. Laboratory evolution of a soluble, self-sufficient, highly active alkane hydroxylase. *Nat. Biotechnol.* 2002, **20**: 1135 - 1139
- 410 30. Farinas ET, Schwaneberg U, Glieder A, Arnold FH. Directed evolution of a cytochrome P450 monooxygenase for alkane oxidation. *Adv. Synth. Catal.* 2001, **343**(6-7): 601-606.
31. Joo H, Lin ZL, Arnold FH. Laboratory evolution of peroxide-mediated cytochrome P450 hydroxylation. *Nature* 1999, **399**(6737): 670-673.
- 415 32. Holtmann D, Hollmann F. The Oxygen Dilemma: A Severe Challenge for the Application of Monooxygenases? *ChemBioChem* 2016, **17**: 1391-1398.
33. Trost BM. The atom economy - A search for synthetic efficiency. *Science* 1991, **254**(5037): 1471-1477.
- 420 34. Choi DS, Ni Y, Fernández-Fueyo E, Lee M, Hollmann F, Park CB. Photoelectroenzymatic oxyfunctionalization on flavin-hybridized carbon nanotube electrode platform. *ACS Catal.* 2017, **7**: 1563-1567.
- 425 35. Ni Y, Fernández-Fueyo E, Baraibar AG, Ullrich R, Hofrichter M, Yanase H, *et al.* Peroxygenase-catalyzed oxyfunctionalization reactions promoted by the complete oxidation of methanol. *Angew. Chem. Int. Ed.* 2016, **55**: 798–801.
- 430 36. Krieg T, Huttmann S, Mangold K-M, Schrader J, Holtmann D. Gas diffusion electrode as novel reaction system for an electro-enzymatic process with chloroperoxidase. *Green Chem.* 2011, **13**: 2686-2689.
37. Kofuji Y, Ohkita S, Shiraishi Y, Sakamoto H, Tanaka S, Ichikawa S, *et al.* Graphitic carbon nitride doped with biphenyl diimide: efficient photocatalyst for hydrogen peroxide production from water and molecular oxygen by sunlight. *ACS Catal.* 2016: 7021-7029.
- 435 38. Hirakawa H, Shiota S, Shiraishi Y, Sakamoto H, Ichikawa S, Hirai T. Au nanoparticles supported on BiVO<sub>4</sub>: effective inorganic photocatalysts for H<sub>2</sub>O<sub>2</sub> production from water and O<sub>2</sub> under visible light. *ACS Catal.* 2016, **6**(8): 4976-4982.
- 440 39. Shiraishi Y, Kofuji Y, Sakamoto H, Tanaka S, Ichikawa S, Hirai T. Effects of surface defects on photocatalytic H<sub>2</sub>O<sub>2</sub> production by mesoporous graphitic carbon nitride under visible light irradiation. *ACS Catal.* 2015, **5**(5): 3058-3066.
- 445 40. Shiraishi Y, Kanazawa S, Sugano Y, Tsukamoto D, Sakamoto H, Ichikawa S, *et al.* Highly selective production of hydrogen peroxide on graphitic carbon nitride (g-C<sub>3</sub>N<sub>4</sub>) photocatalyst activated by visible light. *ACS Catal.* 2014: 774-780.
41. Shiraishi Y, Kanazawa S, Kofuji Y, Sakamoto H, Ichikawa S, Tanaka S, *et al.* Sunlight-driven hydrogen peroxide production from water and molecular oxygen by metal-free photocatalysts. *Angew. Chem. Int. Ed.* 2014, **53**(49): 13454–13459.
- 450 42. Tsukamoto D, Shiro A, Shiraishi Y, Sugano Y, Ichikawa S, Tanaka S, *et al.* Photocatalytic H<sub>2</sub>O<sub>2</sub> production from ethanol/O<sub>2</sub> system using TiO<sub>2</sub> loaded with Au–Ag bimetallic alloy nanoparticles. *ACS Catal.* 2012, **2**(4): 599-603.
- 455 43. Buchalska M, Kobielski M, Matuszek A, Pacia M, Wojtyła S, Macyk W. On oxygen activation at Rutile- and Anatase-TiO<sub>2</sub>. *ACS Catal.* 2015, **5**(12): 7424-7431.



44. Teranishi M, Hoshino R, Naya S-I, Tada H. Gold-nanoparticle-loaded carbonate-modified Titanium(IV) oxide surface: visible-light-driven formation of hydrogen peroxide from oxygen. *Angew. Chem. Int. Ed.* 2016, **55**(41): 12773-12777.
45. Teranishi M, Naya S-I, Tada H. In situ liquid phase synthesis of hydrogen peroxide from molecular oxygen using gold nanoparticle-loaded Titanium(IV) dioxide photocatalyst. *J. Am. Chem. Soc.* 2010, **132**(23): 7850-7851.
46. Pita M, Mate DM, Gonzalez-Perez D, Shleev S, Fernandez VM, Alcalde M, *et al.* Bioelectrochemical oxidation of water. *J. Am. Chem. Soc.* 2014, **136**: 5892–5895.
47. Pichat P. *Photocatalysis and water purification: from fundamentals to recent applications*. Wiley-VCH Verlag GmbH & Co. KGaA, 2013.
48. Priebe JB, Radnik J, Lennox AJJ, Pohl MM, Karnahl M, Hollmann D, *et al.* Solar hydrogen production by plasmonic Au-TiO<sub>2</sub> catalysts: impact of synthesis protocol and TiO<sub>2</sub> phase on charge transfer efficiency and H<sub>2</sub> evolution rates. *ACS Catal.* 2015, **5**(4): 2137-2148.
49. Mifsud M, Gargiulo S, Iborra S, Arends IWCE, Hollmann F, Corma A. Photobiocatalytic chemistry of oxidoreductases using water as the electron donor. *Nat. Commun.* 2014, **5**.
50. Churakova E, Kluge M, Ullrich R, Arends IWCE, Hofrichter M, Hollmann F. Specific photobiocatalytic oxyfunctionalization reactions. *Angew. Chem. Int. Ed.* 2011, **50**(45): 10716-10719.
51. Diesen V, Jonsson M. Formation of H<sub>2</sub>O<sub>2</sub> in TiO<sub>2</sub> photocatalysis of oxygenated and deoxygenated aqueous systems: a probe for photocatalytically produced hydroxyl radicals. *J. Phys. Chem. C* 2014, **118**(19): 10083-10087.
52. Moon GH, Kim W, Bokare AD, Sung NE, Choi W. Solar production of H<sub>2</sub>O<sub>2</sub> on reduced graphene oxide-TiO<sub>2</sub> hybrid photocatalysts consisting of earth-abundant elements only. *Energ. Environ. Sci.* 2014, **7**(12): 4023-4028.
53. Li XZ, Chen CC, Zhao JC. Mechanism of photodecomposition of H<sub>2</sub>O<sub>2</sub> on TiO<sub>2</sub> surfaces under visible light irradiation. *Langmuir* 2001, **17**(13): 4118-4122.
54. Dvoranová D, Barbieriková Z, Brezová V. Radical intermediates in photoinduced reactions on TiO<sub>2</sub> (an EPR spin trapping study). *Molecules* 2014, **19**(11): 17279.
55. Schneider J, Matsuoka M, Takeuchi M, Zhang J, Horiuchi Y, Anpo M, *et al.* Understanding TiO<sub>2</sub> photocatalysis: mechanisms and materials. *Chem. Rev.* 2014, **114**(19): 9919-9986.
56. Finkelstein E, Rosen GM, Rauckman EJ. Spin trapping. Kinetics of the reaction of superoxide and hydroxyl radicals with nitrones. *J. Am. Chem. Soc.* 1980, **102**(15): 4994-4999.
57. Marquez LA, Dunford HB. Reaction of compound III of myeloperoxidase with ascorbic acid. *J. Biol. Chem.* 1990, **265**(11): 6074-6078.
58. Bilski P, Reszka K, Bilska M, Chignell CF. Oxidation of the spin trap 5,5-Dimethyl-1-pyrroline N-oxide by singlet oxygen in aqueous solution. *J. Am. Chem. Soc.* 1996, **118**(6): 1330-1338.
59. Hanaor DAH, Sorrell CC. Review of the anatase to rutile phase transformation. *J. Mat. Sci.* 2011, **46**(4): 855-874.
60. Fitzpatrick TB, Amrhein N, Macheroux P. Characterization of YqjM, an old yellow enzyme homolog from *Bacillus subtilis* involved in the oxidative stress response. *J. Biol. Chem.* 2003, **278**(22): 19891-19897.

61. Hanefeld U, Gardossi L, Magner E. Understanding enzyme immobilisation. *Chem. Soc. Rev.* 2009, **38**(2): 453-468.
- 520 62. Poraj-Kobielska M, Peter S, Leonhardt S, Ullrich R, Scheibner K, Hofrichter M. Immobilization of unspecific peroxygenases (EC 1.11.2.1) in PVA/PEG gel and hollow fiber modules. *Biochem. Eng. J.* 2015, **98**(0): 144-150.
- 525 63. Roots R, Okada S. Estimation of life times and diffusion distances of radicals involved in X-ray-induced DNA strand breaks or killing of mammalian cells. *Rad. Res.* 1975, **64**(2): 306-320.
64. Guo Q, Yue Q, Zhao J, Wang L, Wang H, Wei X, *et al.* How far can hydroxyl radicals travel? An electrochemical study based on a DNA mediated electron transfer process. *Chem. Commun.* 2011, **47**(43): 11906-11908.
- 530 65. Peter S, Karich A, Ullrich R, Grobe G, Scheibner K, Hofrichter M. Enzymatic one-pot conversion of cyclohexane into cyclohexanone: Comparison of four fungal peroxygenases. *J. Mol. Catal. B: Enzym.* 2014, **103**: 47-51.
- 535 66. Kluge M, Ullrich R, Scheibner K, Hofrichter M. Stereoselective benzylic hydroxylation of alkylbenzenes and epoxidation of styrene derivatives catalyzed by the peroxygenase of *Agrocybe aegerita*. *Green Chem.* 2012, **14**(2): 440-446.
- 540 67. Peter S, Kinne M, Wang XS, Ullrich R, Kayser G, Groves JT, *et al.* Selective hydroxylation of alkanes by an extracellular fungal peroxygenase. *FEBS J.* 2011, **278**(19): 3667-3675.
68. Sehl T, Hailes HC, Ward JM, Wardenga R, von Lieres E, Offermann H, *et al.* Two steps in one pot: enzyme cascade for the synthesis of nor(pseudo)ephedrine from inexpensive starting materials. *Angew. Chem. Int. Ed.* 2013, **52**: 6772-6775.
- 545 69. Hailes HC, Rother D, Muller M, Westphal R, Ward JM, Pleiss J, *et al.* Engineering stereoselectivity of ThDP-dependent enzymes. *FEBS J.* 2013, **280**(24): 6374-6394.
- 550 70. Höhne M, Schätzle S, Jochens H, Robins K, Bornscheuer UT. Rational assignment of key motifs for function guides in silico enzyme identification. *Nat. Chem. Biol.* 2010, **6**(11): 807-813.
71. Hanson RL, Davis BL, Chen YJ, Goldberg SL, Parker WL, Tully TP, *et al.* Preparation of (R)-amines from racemic amines with an (S)-amine transaminase from *Bacillus megaterium*. *Adv. Synth. Catal.* 2008, **350**(9): 1367-1375.
- 555 72. Both P, Busch H, Kelly PP, Mutti FG, Turner NJ, Flitsch SL. Whole-cell biocatalysts for stereoselective C–H amination reactions. *Angew. Chem. Int. Ed.* 2016, **55**(4): 1511-1513.
- 560 73. Dong JJ, Fernandez-Fueyo E, Li J, Guo Z, Renirie R, Wever R, *et al.* Halofunctionalization of alkenes by vanadium chloroperoxidase from *Curvularia inaequalis*. *Chem Commun* 2017, **53**: 6207-6210.
74. Fernández-Fueyo E, Younes SHH, Rootselaar Sv, Aben RWM, Renirie R, Wever R, *et al.* A biocatalytic Aza-Achmatowicz reaction. *ACS Catal* 2016, **6**: 5904–5907.
- 565 75. Fernández-Fueyo E, van Wingerden M, Renirie R, Wever R, Ni Y, Holtmann D, *et al.* Chemoenzymatic halogenation of phenols by using the haloperoxidase from *Curvularia inaequalis*. *ChemCatChem* 2015, **7**: 4035-4038.
- 570 76. van Schijndel J, Vollenbroek E, Wever R. The chloroperoxidase from the fungus *Curvularia inaequalis* - a novel vanadium enzyme. *Biochim. Biophys. Acta* 1993, **1161**(2-3): 249-256.
77. Frank A, Seel CJ, Groll M, Gulder T. Characterization of a cyanobacterial haloperoxidase and evaluation of its biocatalytic halogenation potential. *ChemBioChem* 2016, **17**(21): 2028-2032.

- 575 78. Getrey L, Krieg T, Hollmann F, Schrader J, Holtmann D. Enzymatic halogenation of the phenolic monoterpenes thymol and carvacrol with chloroperoxidase. *Green Chem.* 2014, **16**: 1104-1108.
79. Wischang D, Hartung J. Bromination of phenols in bromoperoxidase-catalyzed oxidations. *Tetrahedron* 2012, **68**(46): 9456-9463.
- 580 80. Wischang D, Hartung J. Parameters for bromination of pyrroles in bromoperoxidase-catalyzed oxidations. *Tetrahedron* 2011, **67**(22): 4048-4054.
- 585 81. Itoh N, Hasan A, Izumi Y, Yamada H. Substrate specificity, regioselectivity and stereospecificity of halogenation reactions catalyzed by non-heme-type bromoperoxidase from *Corallina pilulifera*. *Eur. J. Biochem.* 1988, **172**(2): 477-484.
- 590 82. Martin DJ, Qiu K, Shevlin SA, Handoko AD, Chen X, Guo Z, *et al.* Highly efficient photocatalytic H<sub>2</sub> evolution from water using visible light and structure-controlled graphitic carbon nitride. *Angew. Chem. Int. Ed.* 2014, **53**(35): 9240-9245.
83. Zhang W, Bariotaki A, Smonou I, Hollmann F. Visible-light-driven photooxidation of alcohols using surface-doped graphitic carbon nitride. *Green Chem.* 2017, **19**: 2096-2100.
- 595 84. Liu J, Zhao S, Li C, Yang M, Yang Y, Liu Y, *et al.* Carbon nanodot surface modifications initiate highly efficient, stable catalysts for both oxygen evolution and reduction reactions. *Adv. Energ. Mat.* 2016, **6**(9): 1502039-1502039.
- 600 85. Martindale BCM, Hutton GAM, Caputo CA, Reisner E. Solar hydrogen production using carbon quantum dots and a molecular Nickel catalyst. *J Am Chem Soc* 2015, **137**(18): 6018-6025.
86. Hutton GAM, Reuillard B, Martindale BCM, Caputo CA, Lockwood CWJ, Butt JN, *et al.* Carbon dots as versatile photosensitizers for solar-driven catalysis with redox enzymes. *J Am Chem Soc* 2016, **138**(51): 16722-16730.
- 605 87. Ni Y, Holtmann D, Hollmann F. How green is biocatalysis? To calculate is to know. *ChemCatChem* 2014, **6**(4): 930-943.
- 610 88. Tufvesson P, Lima-Ramos J, Nordblad M, Woodley JM. Guidelines and cost analysis for catalyst production in biocatalytic processes. *Org. Proc. Res. Dev.* 2010, **15**(1): 266-274.